Human Molecular Genetics, 2009, Vol. 18, No. 4 **655–666**
doi:10.1093/hmg/ddn395
Advance Access published on November 20, 2008

Homozygous disruption of *PDZD7* by reciprocal translocation in a consanguineous family: a new member of the Usher syndrome protein interactome causing congenital hearing impairment

Eberhard Schneider[1], Tina Märker[3], Angelika Daser[1], Gabriele Frey-Mahn[1], Vera Beyer[1], Ruxandra Farcas[1], Brigitte Schneider-Rätzke[1], Nicolai Kohlschmidt[1], Bärbel Grossmann[1], Katharina Bauss[3], Ulrike Napiontek[2], Annerose Keilmann[2], Oliver Bartsch[1], Ulrich Zechner[1], Uwe Wolfrum[3] and Thomas Haaf[1,*]

[1]Institute of Human Genetics and [2]Division of Communication Disorders, Department of ORL, Johannes Gutenberg University, Langenbeckstrasse 1, 55131 Mainz, Germany and [3]Department of Cell and Matrix Biology, Institute of Zoology, Johannes Gutenberg University, Johannes von Müllerweg 6, 55128 Mainz, Germany

Received October 6, 2008; Revised and Accepted November 18, 2008

A homozygous reciprocal translocation, 46,XY,t(10;11),t(10;11), was detected in a boy with non-syndromic congenital sensorineural hearing impairment. Both parents and their four other children were heterozygous translocation carriers, 46,XX,t(10;11) and 46,XY,t(10;11), respectively. Fluorescence *in situ* hybridization of region-specific clones to patient chromosomes was used to localize the breakpoints within bacterial artificial chromosome (BAC) RP11-108L7 on chromosome 10q24.3 and within BAC CTD-2527F12 on chromosome 11q23.3. Junction fragments were cloned by vector ligation and sequenced. The chromosome 10 breakpoint was identified within the PDZ domain containing 7 (*PDZD7*) gene, disrupting the open reading frame of transcript *PDZD7*-C (without PDZ domain) and the 5′-untranslated region of transcript *PDZD7*-D (with one PDZ and two prolin-rich domains). The chromosome 11 breakpoint was localized in an intergenic segment. Reverse transcriptase–polymerase chain reaction analysis revealed *PDZD7* expression in the human inner ear. A murine *Pdzd7* transcript that is most similar in structure to human *PDZD7*-D is known to be expressed in the adult inner ear and retina. *PDZD7* shares sequence homology with the PDZ domain-containing genes, *USH1C* (harmonin) and *DFNB31* (whirlin). Allelic mutations in harmonin and whirlin can cause both Usher syndrome (USH1C and USH2D, respectively) and congenital hearing impairment (DFNB18 and DFNB31, respectively). Protein–protein interaction assays revealed the integration of PDZD7 in the protein network related to the human Usher syndrome. Collectively, our data provide strong evidence that *PDZD7* is a new autosomal-recessive deafness-causing gene and also a prime candidate gene for Usher syndrome.

INTRODUCTION

Congenital sensorineural hearing loss (SNHL) is among the most common birth defects, occurring in 1–2 of 1000 live births (1). In addition, it may arise throughout childhood and adulthood. Current research suggests that genetic defects account for at least 50–60% of cases of congenital and childhood-onset SNHL (2,3). Syndromic SNHL contributes to 20–30% of SNHL patients and includes nearly 400 different forms. Although SNHL is associated with these syndromes, it is not necessarily the predominant clinical feature. Some prevalent examples of syndromic forms of deafness are Pendred, Waardenburg 1–4, branchio-oto-renal and Usher 1–3 syndromes (4). The majority (70–80%) of the genetic SNHL has a non-syndromic etiology. As of November 2008, 57 autosomal-dominant (DFNA), 77 autosomal-recessive

*To whom correspondence should be addressed. Tel: +49 6131175790; Fax: +49 6131175690; Email: haaf@humgen.klinik.uni-mainz.de

(DFNB) and 8 X-linked (DFN) loci for non-syndromic hearing loss have been listed in the Hereditary Hearing Loss Homepage (http://webh01.ua.ac.be/hhh). The causative genes at 22 DFNA, 27 DFNB and one DFN loci have already been cloned. These genes encode connexins, transcription factors, potassium channels, cytoskeletal proteins, unconventional myosins, scaffold proteins and other cellular components with auditive functions in the inner ear. Mutations in one particular gene, *GJB2* (DFNB1), account for up to 50% of autosomal-recessive cases of non-syndromic SNHL and up to 30% of sporadic cases (5). Mutations in other deafness genes occur at much lower frequencies.

It is interesting to note that syndromic and non-syndromic forms of deafness can be caused by allelic mutations in the same gene. Usher syndrome is both clinically (three subtypes can be distinguished on the basis of disease onset, severity and progression) and genetically (at least 12 loci) heterogeneous and characterized by SNHL and retinitis pigmentosa (6–8). So far, eight causative genes have been identified, some of which have alleles associated with non-syndromic SNHL. Mutations in myosin VIIa cause USH1B and DFNB2 (9), in harmonin USH1C and DFNB18 (10), in cadherin 23 USH1D and DFNB12 (11) and in whirlin USH2D and DFNB31 (12). The gene products related to Usher syndrome are part of dynamic multiprotein complexes ('Usher syndrome protein interactome') that are essential for pathways in hair cells of the inner ear and photoreceptor cells of the retina (6,7).

The genetic heterogeneity of SNHL renders identification of new disease genes difficult. Most currently known SNHL genes have been found by genetic linkage analyses of families with heritable hearing loss and positional cloning of candidate genes. Another promising strategy is the cytogenetic and molecular characterization of chromosome breakpoints in patients who carry apparently balanced chromosome rearrangements that are either *de novo* or segregating with SNHL. In these cases, the specific chromosome rearrangement that disrupts or deletes a gene(s) and/or disturbs gene regulation forms a visible bridge between the patient's genotype and phenotype. Disease-associated chromosome rearrangements have been successfully used for the identification of causative genes underlying neurogenetic disorders (13–16). We have conducted a systematic search for balanced chromosome rearrangements in children with varying degrees of hearing impairment, who attended a specialist clinic. The offspring of a consanguineous family presented with SNHL and a homozygous reciprocal translocation, 46,XY,t(10;11),t(10;11). Here, we report on the positional cloning of *PDZD7* that encodes a PDZ domain-containing scaffold protein, showing characteristics of previously identified Usher syndrome proteins.

RESULTS

Systematic search for SNHL-associated chromosome rearrangements

In more than 300 patients with congenital forms of non-syndromic hearing impairment, we found five cases with 46,XY,t(1;10)(p31.2;q25.2), 46,XX,der(2;5)(inv5)(p15.3;q23) t(2;5)(q33;p15.3), 46,XX,t(2;12)(p13;p13), 46,XY,t(10;15)(q25.3;q21.2) and 46,XY,t(10;11)(q24.3;q23.3),t(10;11)(q24.3;q23.3), respectively, in which an apparently balanced chromosome rearrangement was associated with SNHL. Because 5/300 (1.7%) are far more than the prevalence which would be expected in newborn populations (17,18), it is plausible to assume that in most of these cases the association between SNHL and chromosome rearrangement is not coincidental. Our results show that chromosome analyses in patient cohorts with genetically heterogeneous, relatively unspecific and/or late-manifesting phenotypes are warranted, because for any disease of interest there may be a small subgroup of patients, in which chromosome rearrangements have created a dominant mutation or unmasked a recessive mutation in an underlying gene(s).

Case report

The index patient described here was introduced to the Division of Communication Disorders at the age of 4 years because of a bilateral moderate SNHL. There was no progression in the next 5 years. Physical examination revealed a normal-appearing and age-based developed boy without any anomalies and dysmorphies. Routine workup included creatinine, blood urea nitrogen, complete blood count, tests for thyroid hormone levels, opthalmological examination including funduscopy and electrocardiogram. The most common autosomal-recessive form of deafness, DFNB1, was excluded by complete sequencing of the *GJB2* gene. Pedigree analysis revealed that the parents are consanguineous (Fig. 1). They have an additional two sons and two daughters and also experienced two spontaneous abortions. Chromosome banding analysis of the index patient revealed two identical balanced reciprocal translocations between the long arms of chromosomes 10 and 11, 46,XY,t(10;11)(q24.3;q23.3), t(10;11)(q24.3;q23.3) (Fig. 2A). Both of his parents (Fig. 2B and C) carry the same translocation in a heterozygous state. The mother reported a mild hearing impairment, which does not require hearing aids. The father also suffered from a mild high frequency hearing impairment; however, he works in a noisy environment. The heterozygous translocation was also found in the couple's four other children, who all hear normally. A funduscopy of the index patient at the age of 8 years did not reveal any signs of tapetoretinal degeneration.

Chromosomal breakpoint mapping

In order to map the translocation breakpoints at higher DNA resolution, we selected region-specific bacterial artificial chromosome (BAC) clones from the database (Supplementary Material, Table S1). Individual BACs from the breakpoint regions were hybridized to the patient's metaphase spreads. BACs RP11-108L7 at 102,666,924–102,848,009 bp and RP11-11122F15 at 102,752,043–102,905,775 bp on chromosome 10q24.3 produced distinct fluorescence *in situ* hybridization (FISH) signals on both derivative chromosomes (Fig. 2D), as expected for breakpoint-spanning clones. This narrowed the chromosome 10q24.3 breakpoint down to ~96 kb between 102,752,043 and 102,848,009 bp (overlapping sequence of BACs RP11-108L7 and RP11-11122F15). The reciprocal breakpoint was localized in BAC CTD-2527F12 at 115,258,420–115,437,399 bp on chromosome 11q23.3

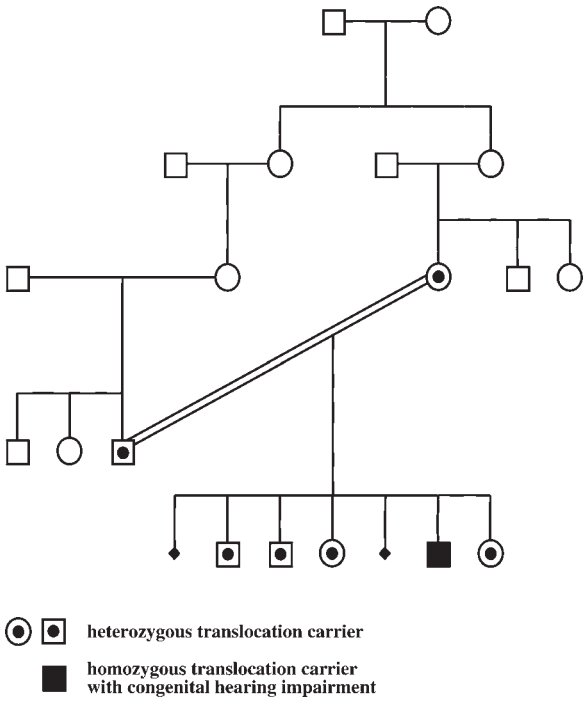

Figure 1. Pedigree of the consanguineous family of the patient with congenital sensorineural hearing impairment and homozygous reciprocal translocation t(10;11)(q24.3;q23.3).

(Fig. 2E). In contrast to CTD-2527F12, the overlapping BACs RP11-188O8 at 115,174,882–115,337,529 and RP11-13C8 at 115,327,799–115,507,934 bp did not produce split hybridization signals, hybridizing only to the der (11) and the der (10), respectively. Because in our experience, 20 kb of genomic DNA sequence is sufficient to generate a detectable FISH signal at the target region, the breakpoint on chromosomes 11q23.3 must lie in the 30 kb interval between 115,317,529 and 115,347,799 bp, including the distal 20 kb of RP11-188O8 and the proximal 20 kb of RP11-13C8.

Database analyses (http://www.ensembl.org and http://www.ncbi.nlm.nih.gov) revealed several genes (*PEO1*, *LZTS2*, *PDZD7*, *SEMA4G*, *MRPL43*, *SFXN3* and *KAZALD*) in the 10q24.3 breakpoint region, whereas no candidate gene was found in the 11q24.3 breakpoint region. However, it is interesting to note that the radixin (*RDX*) gene at the DFNB24 locus (19) lies 5.7 Mb proximal and the tectorin alpha (*TECTA*) gene at the DFNA8/12 (20) and DFNB21 loci (21), respectively, 5.2 Mb distal to the breakpoint on chromosome 11q23.3. We focused our positional cloning efforts on the 10q24.3 breakpoint. To test whether a given candidate gene(s) is disrupted or deleted by t(10;11)(q24.3;q23.3), we designed primers for the polymerase chain reaction (PCR) amplification of ~5 kb fragments from the 10q24.3 breakpoint-spanning BAC (Supplementary Material, Table S2). Fragments 10q24A, C and D could be amplified from both the patient's genomic DNA and controls. The 5273 bp fragment 10q24B was detectable in the heterozygous translocation carriers, but not in the index patient (Fig. 3A), as expected for a breakpoint-spanning fragment. To narrow down the breakpoint region further, we subdivided the 5273 bp fragment in smaller PCR fragments. By PCR typing of the patient and his brother, the breakpoint was localized to the 564 bp fragment 10q24B4.2 (Fig. 3B) in intron 10 of the PDZ domain-containing protein 7 (*PDZD7*) gene (Fig. 3C).

Breakpoint cloning

By using a vector ligation technique, it was possible to clone a junction fragment from the derivative chromosome 11. T7 forward primer and a *PDZD7* reverse primer (Supplementary Material, Table S2), which binds to the 564 bp breakpoint-containing segment on chromosome 10q24.3, produced the expected ~650 bp fragment (insert plus 90 bp of vector sequence) from control DNA and an ~1400 bp fragment from patient DNA (Fig. 4A). The heterozygous brother of the patient displayed both the 650 and the 1400 bp fragment (data not shown). Sequencing of this junction fragment 1 revealed a fusion sequence between an intergenic segment from chromosome 11q23.3 (breakpoint at 115,319,661+, Ensembl release 48) and the *PDZD7* gene on chromosome 10q24.3 (102,764,759+; Ensembl release 48) (Fig. 4B). Junction fragment 1 consists of 90 bp of vector, 987 bp of chromosome 11 and 339 bp of chromosome 10 sequence and is derived from the der (11). The now available sequence information from both breakpoint regions allowed us to design a forward primer on chromosome 10q24.3 and a reverse primer on chromosome 11q23.3 (Supplementary Material, Table S2) for the amplification of the reciprocal junction fragment 2 (159 bp of chromosome 10 and 1514 bp of chromosome 11 sequence) from the der (10) (Fig. 4C). Sequencing of junction fragment 2 revealed identical breakpoint localizations on chromosomes 10 (102,764,759+) and 11 (115,319,661+). Evidently, the chromosome breakage and fusion events were not associated with DNA loss in the breakpoint regions. Bioinformatical (BioEdit) analysis (http://www.mbio.ncsu.edu/BioEdit/BioEdit.html) of the t(10;11)(q24.3;23.3) fusion sequence did not provide any evidence for the existence of a PDZD7 fusion protein.

Transcripts and protein isoforms of *PDZD7*

The *PDZD7* gene is 23.3 kb long and consists of 16 exons (Fig. 5A). There are four known protein-coding transcripts, which—for the sake of simplicity—are called *PDZD7*-A, -B, -C and -D (Fig. 5B). *PDZD7*-A and *PDZD7*-B use only exons upstream of the breakpoint and therefore may be unaffected. The corresponding protein isoforms are endowed with a tandem of two PDZ domains (Fig. 5C). PDZ1 is encoded by genomic exon 3 (7091–7657 bp) and corresponds to amino acids 86–168; PDZ2 is encoded by genomic exon 4 (8830–10 463 bp) and corresponds to amino acids 210–293. The breakpoint in intron 10 disrupts the open reading frame of transcript *PDZD7*-C, which encodes a protein isoform without PDZ domain, as well as the 5′-untranslated region (UTR) of transcript *PDZD7*-D, which encodes a proline-rich protein with one PDZ domain. The PDZ domain of PDZD7-D is encoded by genomic exons 14–16 (20 828–22 374 bp) and corresponds to amino acids 223–295.

Sequence comparisons revealed that the PDZ domains of isoforms PDZD7-A and B, which are very similar in structure,

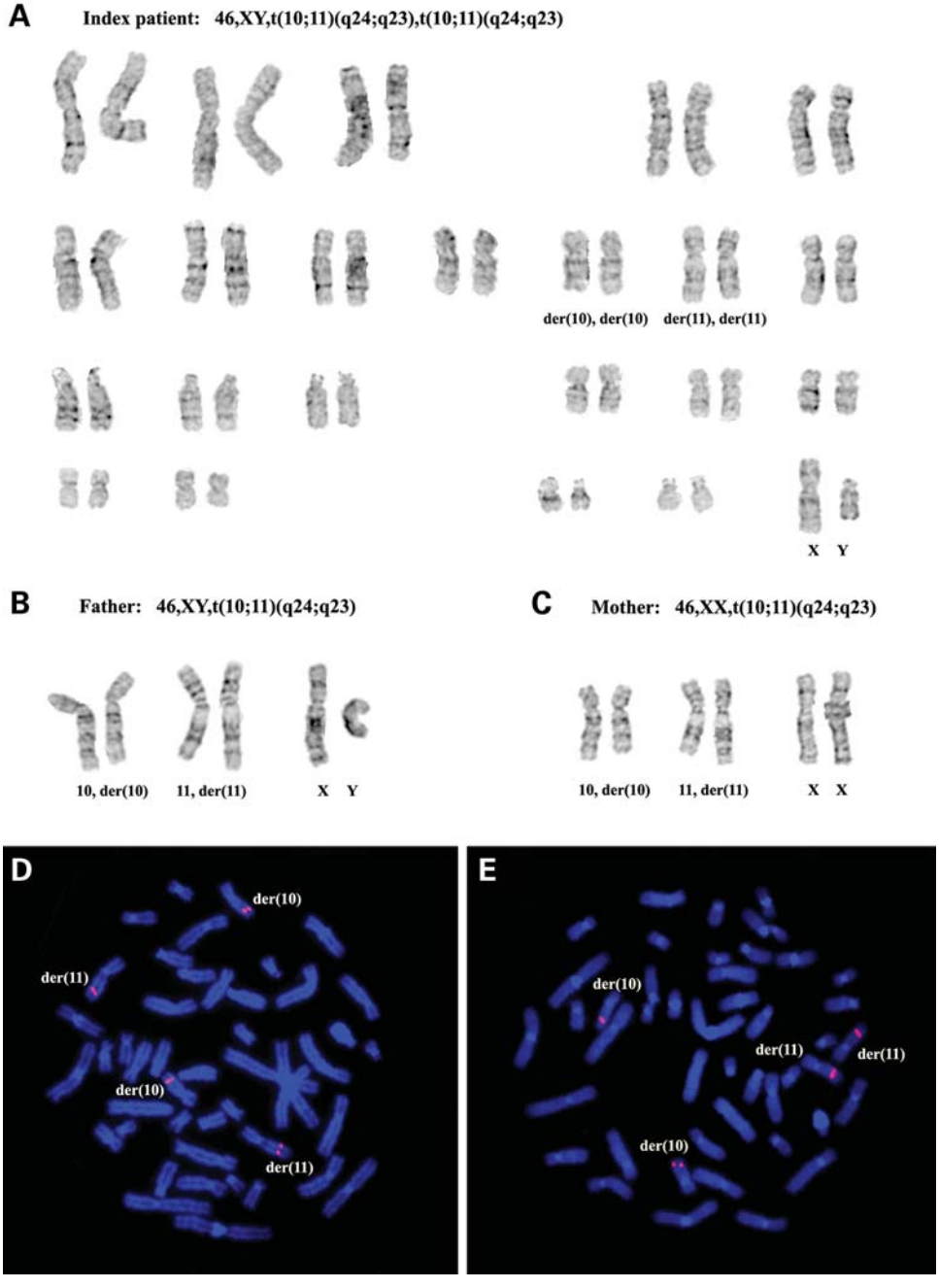

Figure 2. Cytogenetic and molecular cytogenetic characterization of the t(10;11)(q24.3;q23.3). (**A**) GTG-banded karyotype of the index patient with homozygous translocation. Partial karyotypes of the patient's father (**B**) and mother (**C**), both carrying the translocation in a heterozygote state. FISH mapping of breakpoint-spanning BAC RP11-108L7 from chromosome 10q24.3 (**D**) and BAC CTD-2527F12 from chromosome 11q23.3 (**E**) on patient's metaphase spreads. The BACs are labeled by tetramethyl-rhodamine in red, and the chromosomes are counterstained with DAPI in blue. Note the split hybridization signals of both BACs on the der (10) and the der (11).

share extensive homology with the PDZ domain-containing proteins whirlin and harmonin (Fig. 6A), which are encoded by the Usher syndrome genes *USH1C* and *DFNB31*. The PDZ domain in the isoform PDZD7-D is also homologous to whirlin and harmonin (Fig. 6B). When we sequenced the coding regions of the *PDZD7* gene in a healthy control individual, we noted an in-frame insertion of 6 nt encoding for an arginine (R) and a serine (S) in exon 14, compared with the wild-type (chromosome 10: 102,758,214–102,761,691) (Fig. 7). The insertion occurred in a stretch of seven arginine–alanine repeats in a proline-rich region of the PDZ domain-containing isoform PDZD7-D. Genotyping of 10 controls revealed the wild-type sequence in seven individuals and the insertion polymorphism, which is not yet listed in the current databases of genomic variants, in three individuals. In this context, it is interesting to note that the expanded

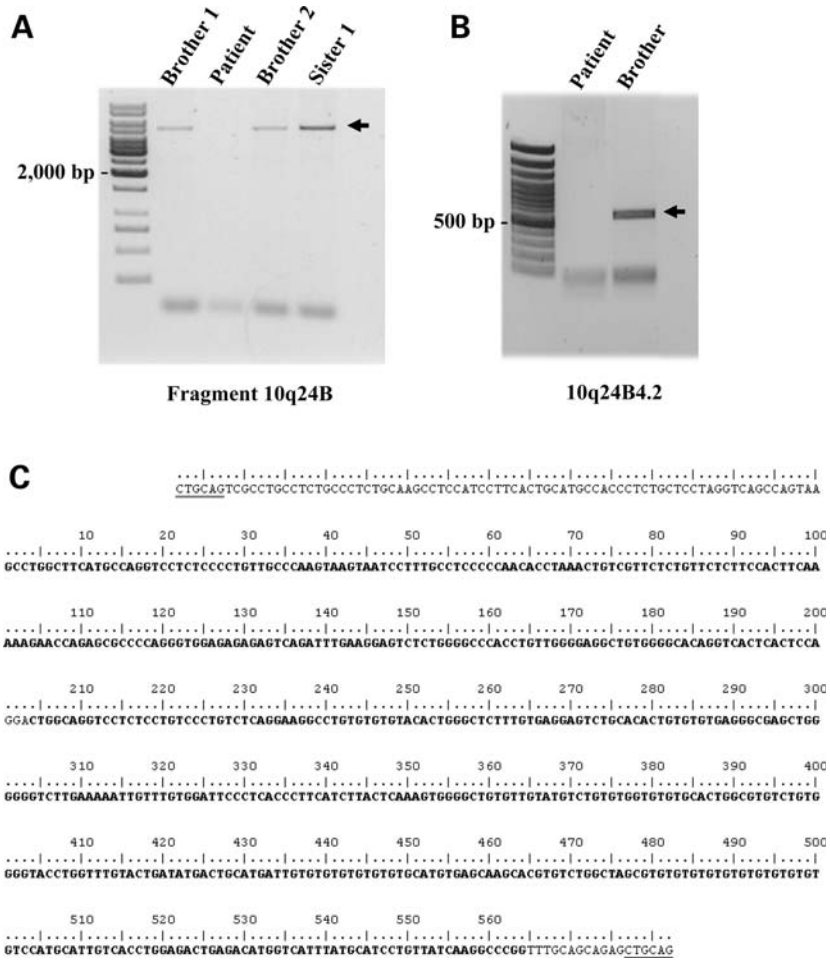

Figure 3. PCR mapping of the chromosome 10q24.3 breakpoint. (**A**) The breakpoint-spanning 5273 bp fragment 10q24B (arrow) is amplified from the patient's two brothers and older sister, who are heterozygous translocation carriers, but not from the homozygous patient. (**B**) The breakpoint-spanning 564 bp fragment 10q24B4.2 (arrow) is amplified from a heterozygous brother, but not from the patient. (**C**) Sequence of the breakpoint-spanning region in intron 10 of the *PDZD7* gene. Sequence homologous to the 564 bp fragment is highlighted in bold. The underlined bases in the upstream and downstream sequences indicate *Pst*I restriction sites for vector ligation.

repeat with eight arginine–alanine motifs corresponds to the chimpanzee and orangutan wild-type. The rhesus macaque is endowed with only six repeats. The bushbaby as a primitive primate, and the mouse as an outgroup showed shorter imperfect repeats. Whether this intra- and inter-specific insertion–deletion polymorphism affects the binding properties of PDZD7 remains to be elucidated.

Tissue expression analyses of *PDZD7*

According to the NCBI/UniGene/ESTProfileViewer (http://www.ncbi.nlm.nih.gov/UniGene/ESTProfileViewer.cgi?uglist=Hs.438245), the human *PDZD7* gene is expressed in numerous tissues and organs including brain. However, there are no data on expression in the inner ear. We used exon-spanning primers (Supplementary Material, Table S2), which detect all four known transcripts, to study the *PDZD7* expression in adult human inner ear and cortex. Primers for *ACTB* and *GAPDH* were used as controls. The expected 298 bp *PDZD7* reverse transcriptase (RT)–PCR product was easily amplified from cortex total RNAs, whereas only weak bands were produced from several independent whole inner ear samples (data not shown). The corresponding genomic DNA fragment would be 822 bp long. To exclude an artifact, the weak 298 bp band from inner ear was gel-extracted, re-amplified and sequence-verified. Our data suggest that *PDZD7* is weakly expressed in the adult human inner ear or, more likely, only expressed in few specialized cells of the inner ear. The murine *Pdzd7* transcript NM 177605.3, which is known to be expressed in the inner ear and retina (NCBI/UniGene/EST-ProfileViewer), shares the highest structural similarity with the human PDZ domain-containing transcript *PDZD7*-D, which is disrupted by t(10;11)(q24.3;23.3).

Direct binding of PDZD7 to Usher syndrome scaffold proteins

The expression profile including the inner ear and retina together with the structural and functional homology of the PDZD7 protein to harmonin and whirlin prompted us to evaluate PDZD7 in the Usher syndrome protein network (22–25). In order to validate the interaction between PDZD7 and the

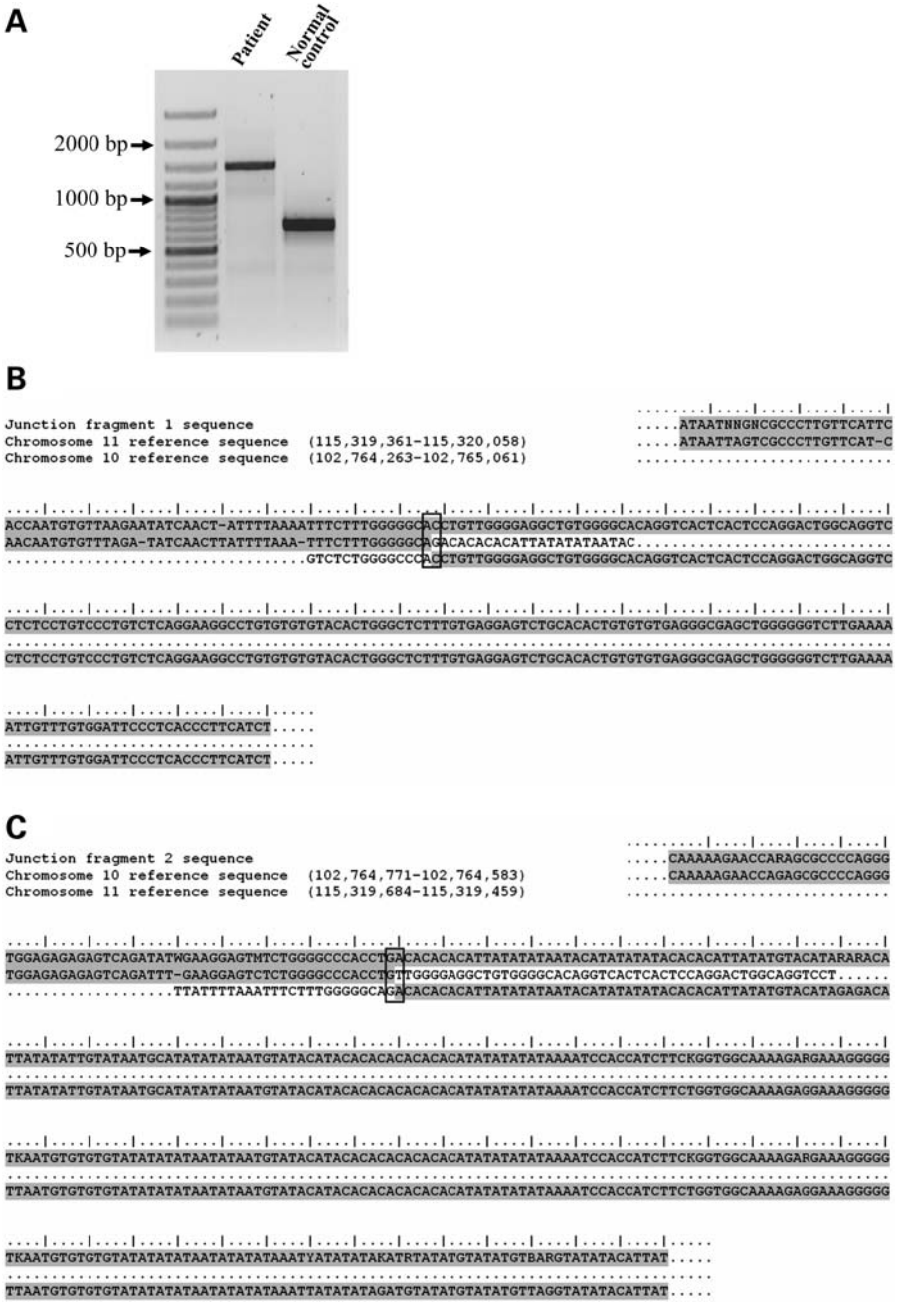

Figure 4. Cloning and sequencing of the t(10;11)(q24.3;q23.3) junction fragments. (**A**) Amplification of PCR fragments from *Pst*I-digested genomic DNA ligated into pBluescriptII, using a vector-specific and a chromosome 10q24.3-specific primer. Genomic DNA of the homozygous patient produced a ~1400 bp junction fragment 1, whereas control DNA yielded the expected ~650 bp fragment from chromosome 10q24.3. (**B**) Comparison of the junction fragment 1 sequence with the human chromosome 11 and 10 reference sequences revealed that it is derived from the der (11) and localized the breakpoint (indicated by a frame) to basepair 115,319,661+ on chromosome 11 and 102,764,759+ on chromosome 10. Homologous sequences are shaded in gray. (**C**) Sequencing of the reciprocal junction fragment 2 from the der (10) confirmed the breakpoint localizations on chromosomes 10 and 11.

Usher syndrome type 1 G (USHG1) protein SANS (scaffold protein containing ankyrin repeats and SAM domain), we adopted recombinant expressed domains of both proteins in gluthatione *S*-transferase (GST) pull-down assays. Immobilized GST-tagged PDZD7 pulled down FLAG-tagged full-length SANS from HEK293T cell lysates. In western blot analysis with anti-FLAG, we identified a single band at ~57 kDa, the estimated molecular weight of 3xFLAG-SANS, indicating the direct binding of PDZD7 to SANS (Fig. 8A). In contrast, GST alone pulled down only a very fade band of 3xFLAG-SANS. For testing the incorporation of PDZD7 in Usher syndrome protein networks in the retina, we adopted GST-tagged PDZD7 or GST alone to protein lysates of the mouse retina and probed the western blot with anti-harmonin. Quantification of the detected bands revealed that four times more harmonin was pulled down from the retinal-expressed

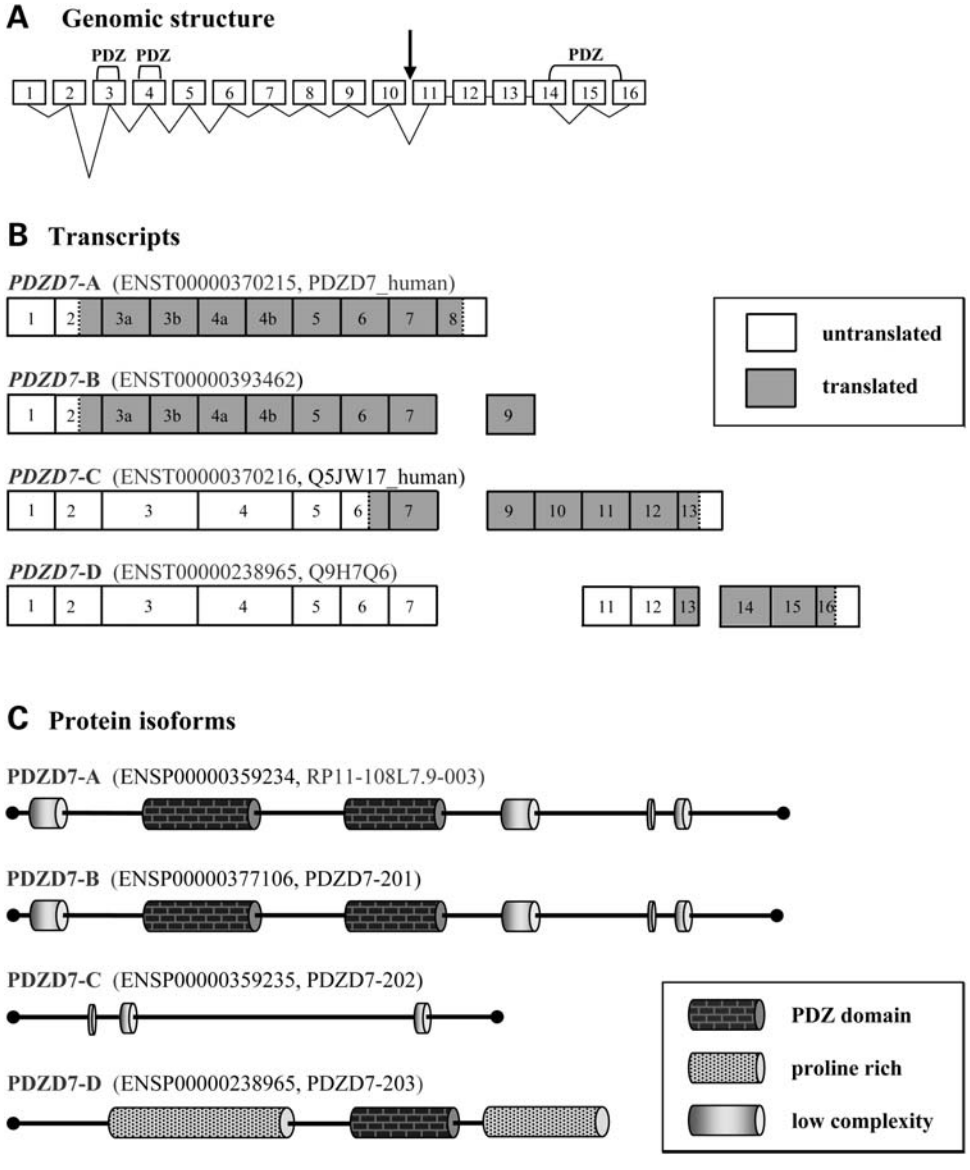

Figure 5. Genomic structure of *PDZD7* and known protein-coding transcripts. (**A**) The human *PDZD7* gene consists of 16 exons that form four different transcripts. The vertical arrow indicates the translocation breakpoint in intron 10. (**B**) Transcripts *PDZD7*-A (ENST00000370215, PDZD7_human) and *PDZD7*-B (ENST00000393462) split the genomic exons 3 and 4 into two smaller exons each and differ only in their 3′-ends. They use only exons upstream of the translocation breakpoint. Transcript *PDZD7*-C (ENST00000370216, Q5JW17_human) and *PDZD7*-D (ENST00000238965, Q9H7Q6) are disrupted in the open reading frame and the 5′-UTR, respectively. (**C**) Protein isoforms PDZD7-A (ENSP00000359234, RP11-108L7.9-003) and PDZD7-B (ENSP00000377106, PDZD7-201) contain two tandemly arrayed PDZ domains each. PDZD7-C (ENSP00000359235, PDZD7-202) does not contain a PDZ domain, whereas PDZD7-D (ENSP00000238965, PDZD7-203) contains one PDZ and two prolin-rich domains.

proteins with GST-tagged PDZD7 than with GST alone (Fig. 8B). All known characteristics of PDZD7 and its interaction with Usher syndrome scaffold proteins suggest PDZD7 as a further component of the Usher syndrome protein network in cochlear hair cells and retinal photoreceptor cells.

DISCUSSION

The pedigree of the consanguineous family with a homozygous reciprocal translocation carrier, 46,XY,t(10;11),t(10;11) is consistent with an autosomal-recessive form of deafness caused by disruption of the *PDZD7* gene in the chromosome 10q24.3 breakpoint region. The second breakpoint on chromosome 11q23.3 lies in relatively close proximity to two other non-syndromic deafness genes, *RDX* (DFNB24) (19) and *TECTA* (DFNA8/12 and DFNB21) (20,21), although the >5 Mb distance makes a position effect on *RDX* and/or *TECTA* expression unlikely. The Usher syndrome genes *CDH23* (USH1D) and *PCDH15* (USH1F) lie 29.5 and 46.5 Mb, respectively, proximal to the 10q24.3 breakpoint, whereas *MYO7A* (USH1B) and *USH1C* lie 38.7 and 97.8 Mb proximal to the 11q23.3 breakpoint (http://webh01.ua.ac.be/hhh). Expression of some genes can be influenced by

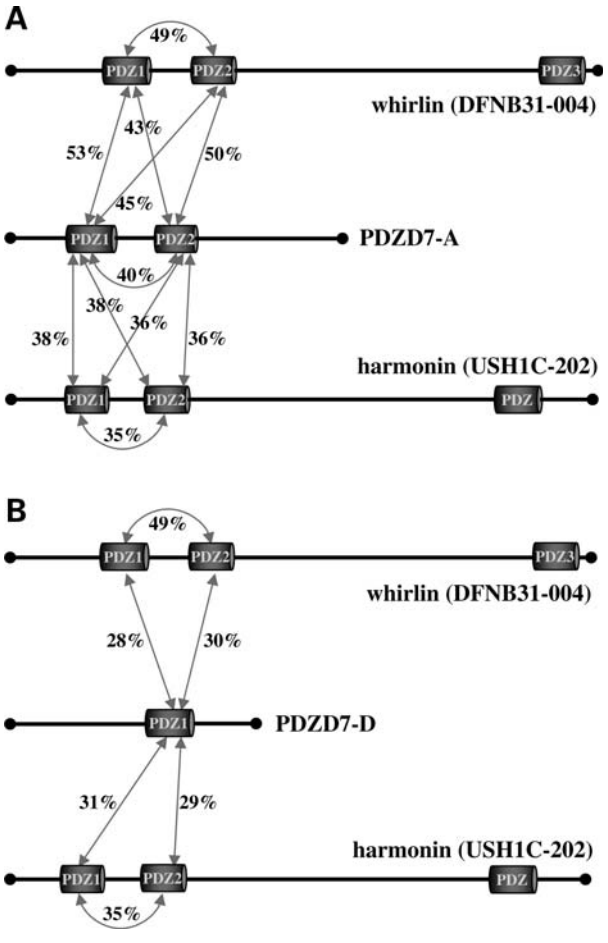

Figure 6. Amino acid sequence similarity of PDZD7 with whirlin and harmonin. Comparison of the PDZ domain containing isoforms PDZD7-A (**A**) and PDZD7-D (**B**) with whirlin and harmonin. The arrows between two given PDZ domains indicate the percentage of amino acid sequence similarity.

regulatory elements well outside the transcription and promoter regions (26). In a number of human developmental disorders, including X-linked deafness (misregulation of *POU3F4*) (13), holoprosencephaly (*SHH*) (27), preaxial polydactyly (*SHH*) (28), campomelic dysplasia (*SOX9*) (29,30) and Pierre–Robin sequence (*SOX9* and *KCNJ2*) (31), it has been shown that the distance of the disease-causing chromosome breakpoint and/or microdeletion to the 3′ or 5′ end of the misregulated gene can be over 1 Mb. However, so far there is no evidence for position effects at >2 Mb distance from the breakpoint region.

Although this may be a chance coincidence, it is tempting to speculate that the localization of essential genes for the function of inner ear hair cell stereocilia at both breakpoint regions, *PDZD7* at 10q24.3 and *RDX* and *TECTA* within a 5 Mb interval at 11q23.3, is the consequence of higher-order nuclear organization. The 'contact-first' hypothesis of the formation of chromosome rearrangements assumes that DNA repair joins ends from different DNA damage-induced double-strand breaks that were closely juxtaposed in the interphase nucleus at the time when the DNA damaging event occurred (32,33). There is a highly dynamic nuclear architecture that may have a function in the regulation of gene expression (34). Genes on different chromosomes, i.e. *PDZD7*, *RDX* and *TECTA*, that are co-ordinately expressed/regulated and work together in a single biological module may be non-randomly physically associated in the nucleus (35), facilitating DNA damage-induced illegitimate recombination events.

Homozygosity for translocations is very rare. Most published cases are homozygous Robertsonian translocations with $2n = 44$ chromosomes, including rob(13;14),rob(13;14) (36,37) and rob(14;21),rob(14;21) (38,39). There are four reports on homozygous reciprocal translocations, namely, der(22)t(Y;22),der(22)t(Y;22) (40), t(3;16),t(3;16) (41), t(17;20),t(17;20) (42) and t(7;12),t(7;12) (43), all in the offspring of consanguineous parents. The phenotype of cortical lissencephaly with cerebellar hypoplasia in two siblings with t(7;12),t(7;12) is explained by the homozygous disruption of the reelin gene at 7q22.1. This clearly demonstrates that rare homozygous translocations can be used to identify recessive disease gene mutations.

Several lines of evidence suggest that biallelic inactivation of *PDZD7* can cause non-syndromic hearing impairment. In our index patient suffering from congenital SNHL, both *PDZD7* alleles are disrupted by homozygous reciprocal translocation, whereas heterozygous translocation carriers either hear normally or display only mild hearing impairment as adults. Although we cannot totally exclude that environmental factors are responsible for the observed mild hearing impairment of the parents, it is well possible that *PDZD7* haploinsufficiency predisposes to adulthood-onset or old age hearing impairment. The chromosome 10q24.3 breakpoint creates a loss of function mutation. One of the disrupted PDZD7 isoforms is structurally and functionally related to the PDZ domain-containing scaffold proteins harmonin and whirlin, which play a central role in the Usher syndrome protein network. Genetically heterogeneous diseases such as Usher syndrome and Fanconi anemia provide good examples that mutations in functionally related genes, i.e. genes in the same multiprotein complex and/or biochemical pathway, lead to the same or similar phenotypes (6,44,45).

Pull-down experiments support the idea of an integration of PDZD7 into the protein interactome related to Usher syndrome, indicating that PDZD7 is a prime candidate for human Usher syndrome. Examination of our index patient did not show any signs of retinitis pigmentosa or vestibular dysfunction at the age of 8 years. Although we cannot exclude the possibility that he will develop additional symptoms later in life, it is more likely that homozygous disruption of intron 10 of *PDZD7* in our patient causes non-syndromic hearing impairment. Similar to harmonin (*USH1C*) and whirlin (*DFNB31*), more severe mutations in *PDZD7* (interfering with all four known transcripts) may cause Usher syndrome. Nevertheless, the clinical phenotype (non-syndromic SNHL) caused by biallelic inactivation of *PDZD7* is consistent with its relation with harmonin and whirlin at the gene and protein levels.

Both scaffold proteins harmonin and whirlin strongly contribute to the organization of protein networks, integrating the function of all other Usher syndrome proteins (6,22–25,46–48). In this Usher syndrome protein interactome, both proteins directly bind with their PDZ domains the motor protein myosin VIIa (USH1B), the Usher cadherins, cadherin

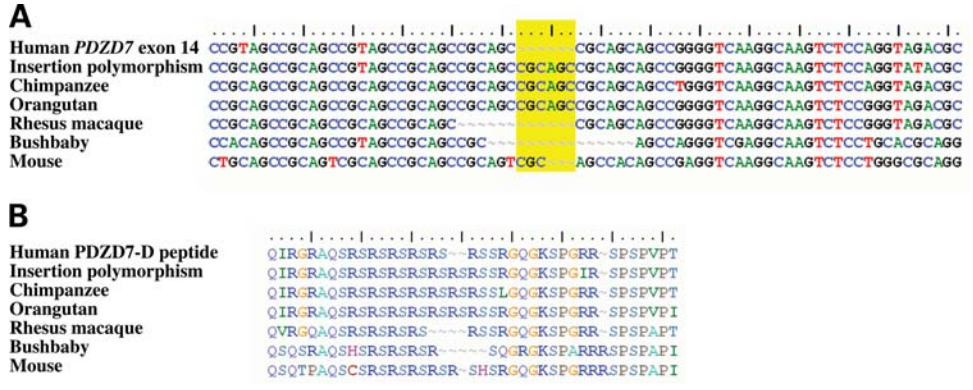

Figure 7. Insertion–deletion polymorphism in exon 14 of *PDZD7*. (**A**) Nucleotide sequence alignment of human wild-type *PDZD7* exon 14 and the identified insertion polymorphism with the chimpanzee, orangutan, rhesus macaque, bushbaby and mouse genomic reference sequences. (**B**) Amino acid sequence alignment of human isoform PDZD7-D, human insertion polymorphism, chimpanzee, orangutan, rhesus macaque, bushbaby and mouse.

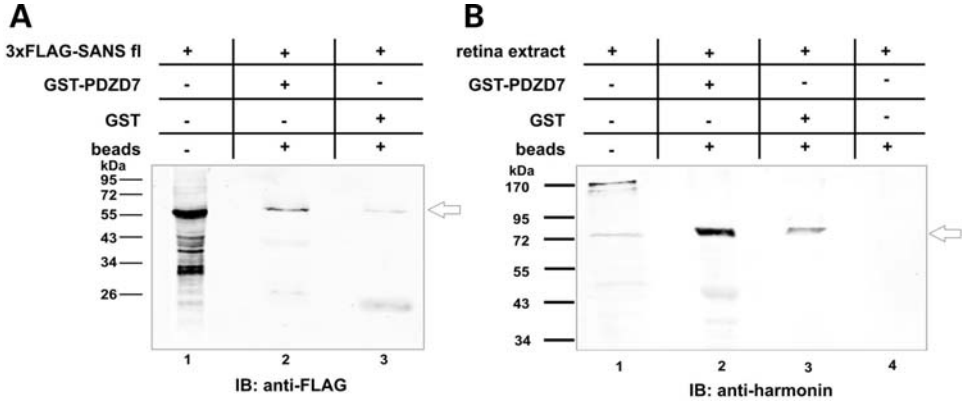

Figure 8. Validation of the PDZD7 integration into the Usher syndrome protein network. (**A**) Validation of the SANS–PDZD7 interaction by GST pull-down analyses. The lysate of HEK293T cells transiently transfected with 3×FLAG-SANS (lane 1, 10% of input) was incubated with GST-PDZD7 (lane 2) or GST alone (lane 3). Anti-FLAG western blot analysis revealed a prominent band at ∼57 kDa, resembling the ascertained molecular weight of 3×FLAG-SANS (arrow), pulled down by GST-PDZD7. In contrast, a very fade band was observed in pull downs with GST alone. (**B**) PDZD7 interaction with harmonin in the mouse retina validated by GST pull-down assay. Murine retina extract (lane 1, 15% of input) was incubated with immobilized full GST-PDZD7 (lane 2), GST (lane 3) or sepharose beads alone (lane 4). Anti-harmonin revealed a band of ∼72 kDa (lane 2), the ascertained molecular weight of the abundant splice variant harmonin a1 (arrow), pulled down by GST-PDZD7. A 4-fold weaker band is detected in the control incubated with GST alone (lane 3). No signal was observed in the sepharose bead control (lane 4). For quantification, intensities of the 72 kDa band were assigned by an Odyssey infra red imaging system: lane 1, 0.36; lane 2, 3.95; lane 3, 0.99.

23 (USH1D) and procadherin 15 (USH1F), the scaffold protein SANS (USH1G), the transmembrane protein USH2A and the very large G protein-coupled receptor, VLGR1b/GRP98 (USH2C). In the inner ear, this multiprotein network is assembled mainly in stereocilia and synaptic regions of hair cells. There Usher syndrome protein networks are essential for the development of stereocilia, the synaptic function and the mechano-electric transduction (6,7). In retinal photoreceptor cell networks, Usher syndrome proteins are found at synapses in the periciliary region, indicating a close relation to other ciliopathies (7,25). Based on the characteristics of *PDZD7*, its expression in the inner ear and interaction of the PDZD7 protein with SANS (USH1G) and with harmonin (USH1C) from retinal origin, we conclude that it is another PDZ domain-containing partner in the Usher interactome, which may participate in the development of stereocilia in hair cells and in ciliary functions in retinal photoreceptor cells. Certainly, *PDZD7* is a very good candidate gene for a novel human Usher syndrome locus.

MATERIALS AND METHODS

Cytogenetic and molecular cytogenetic analyses

Metaphases were prepared from short-term phytohemagglutinin-stimulated lymphocyte cultures and analysed with classic GTG banding at the 500 band level. Region-specific BAC clones for FISH mapping were selected from the Wellcome Trust Sanger Institute Ensembl contigs (http://www.ensembl.org) and the UCSC Genome Browser (http://genome.ucsc.edu) (Supplementary Material, Table S1). Genomic BAC DNAs were labeled with fluorescein-12-dUTP or tetramethyl-rhodamine-5-dUTP (Roche Diagnostics, Mannheim, Germany) by standard nick translation. FISH was

performed on the patient's metaphase spreads, as described previously (14,49).

PCR analyses

All PCRs were performed according to standard protocols. The reaction mixture consisted of 2.5 μl 10× PCR buffer, 2.5 μl 50 mM $MgCl_2$, 2.5 μl 10 mM dNTP mix, 1.0 μl (100 ng) of each forward and reverse primer, 0.5 μl (2.5 U) Taq polymerase, 14 μl PCR-grade water and 100 ng template DNA. PCR amplifications were carried out with an initial denaturation step at 94°C for 3 min, 35 cycles of 94°C for 30 s, primer-specific annealing temperature for 30 s, 72°C for 60 s and a final extension step at 72°C for 10 min. In order to amplify larger (~5 kb) fragments from the 10q24.3 breakpoint region, the Expand Long Template PCR System (Roche Diagnostics) was used according to the recommendations of the manufacturer with a series of primer pairs (Supplementary Material, Table S2) chosen from the genomic sequence of breakpoint-spanning BAC clone RP11-108L7. The PCR reaction contained 10 μl 5× Expand Long Range Buffer with 12.5 mM $MgCl_2$, 2.4 μl nucleotide mix, 1.5 μl (150 ng) each of forward primer and reverse primer, 0.7 μl (3.5 U) Expand Long Range Enzyme mix, 100 ng template DNA and 33 μl water. Annealing temperatures and elongation times were optimized for each primer pair.

Vector ligation

A new vector ligation technique was used to clone a junction fragment of the t(10;11)(q24.3;23.3) translocation. Genomic DNA of the index patient with homozygous translocation, of his brother with heterozygous translocation and a control person with normal karyotype was digested with *Pst*I. This restriction enzyme was chosen because it cuts nearby but not within the chromosome 10q24.3 breakpoint-containing 564 bp segment. Because there is a *Pst*I restriction site approximately every 1000 bp in the human genome sequence, the *Pst*I-digested junction fragment can be expected to be 1000–2000 bp in size. Two micrograms of genomic DNA each and 2.0 μl pBluescriptII phagemid vector DNA were digested in a 40 μl reaction containing 1.5 μl *Pst*I (New England Biolabs, Frankfurt/Main, Germany), 4 μl 10× NEBuffer 3 and PCR-grade water. Following incubation at 37°C overnight, the enzyme was inactivated at 80°C for 20 min. To remove 5′-phosphate residues, the plasmid vector was treated with calf intestinal alkaline phosphatase (New England Biolabs). Digested genomic DNA and vector DNA were ligated together at 16°C overnight using 1 μl plasmid vector, 10 μl (~500 ng) target DNA, 12.5 μl T4 DNA ligase 2× rapid ligation buffer and 1.5 μl T4 DNA ligase (Promega, Mannheim, Germany). The reaction was stopped by incubation at 75°C for 20 min. The ligation products were cleaned with DNA Clean & Concentrator 5 (Zymo Research, Orange, CA, USA). The pBluesciptII vector contains T7 and M13 primer-binding sites. Different combinations of vector and insert (breakpoint-spanning fragment) primers (Supplementary Material, Table S2) were used to amplify a junction fragment from the plasmid library.

DNA sequencing

Following Exo/SAP digestion, dye terminator cycle sequencing of the PCR products was carried out using the CEQ DTCS Quick Start Kit (Beckman Coulter, Krefeld, Germany). Sequencing products were separated on a Beckman Coulter CEQ 8000 Genetic Analysis System. The BLAST program (http://www.ensembl.org/Homo_sapiens/blastview and http://www.ncbi.nlm.nih.gov/BLAST) was used to analyze the sequencing data.

Expression analysis

Total RNAs were extracted from adult inner ear and cortex using TRIZOL reagent (Invitrogen, Karsruhe, Germany). Tissue samples were obtained from male persons between 20 and 45 years within 2 days post-mortem. The samples were frozen immediately after dissection and stored in liquid nitrogen. RNA quality and quantity were determined with a NanoDrop spectrophotometer (Peqlab, Erlangen, Germany). cDNA was synthesized by reverse transcription of total RNA with SuperscriptIII transcriptase (Invitrogen), using the Invitrogen protocol for first strand synthesis. Two microliters of this cDNA was then used as a template in a PCR reaction with primers spanning *PDZD7* exons 6 and 7 (Supplementary Material, Table S2).

GST pull-down assays

Constructs encoding full-length murine *Pdzd7* cDNA (FANTOM 3 clone 9130207N01, imaGenes) were cloned into pDEST15 vector (Gateway Cloning System, Invitrogen). GST-fusion proteins were generated by transforming *Escherichia coli* BL21AI cells with pDEST15-*Pdzd7*. Cells were incubated at 30°C with 0.5 mM isopropyl-β-D-thiogalactopyranoside overnight and subsequently lysed with STE buffer [1% Sarkosyl, 1% Triton X-100, 5 mM dithiothreitol (DTT)], supplemented with complete protease inhibitor cocktail (Roche Diagnostics). Lysates were incubated with gluthathione–sepharose 4B beads (Amersham Biosciences, Freiburg, Germany). The GST-fusion proteins bound to the beads were washed with lysis buffer and TBSTD (TBS with 1% Triton X-100 and 2 mM DTT). The amount of bound GST-fusion protein was verified on a NUPAGE Novex 4–12% bis–tris sodium dodecyl sulfate (SDS)–polyacrylamide gel electrophoresis (PAGE) gel and stained with Simply Blue Safe Stain (Invitrogen).

FLAG-tagged human SANS full-length protein was produced by transfection of HEK293T cells with the appropriate vectors, using a combination of Lipofectamine LTX and PLUS reagent (Invitrogen) according to the manufacturer's instructions. Twenty-four hours after transfection cells were washed with phosphate-buffered saline and subsequently lysed on ice in lysis buffer (50 mM Tris–HCl, pH 7.5, 150 mM NaCl, 0.5% Triton X-100). Retina lysate of mature C57BL/6J mice was prepared in HNTG buffer (20 mM HEPES, 150 mM NaCl, 0.1% Triton X-100, 6 mM EDTA, 10% glycerol, pH 7.4). Cell extracts or retinal extracts were incubated overnight at 4°C with equal amounts of beads preincubated either with GST or with GST fusion protein.

Beads were washed, and precipitated protein complexes were eluted with SDS sample buffer and subjected to SDS–PAGE and western blot analysis.

Western blot analyses

For western blot analyses, samples of GST pull-downs were mixed with SDS–PAGE sample Laemmli buffer (62.5 mM Tris–HCl, pH 6.8, 10% glycerol, 2% SDS, 5% mercaptoethanol, 1 mM EDTA and 0.025 mM Bromphenol blue) and separated on 12% polyacrylamide gels. Subsequently, separated proteins were transferred onto polyvinylidene difluoride membranes (Millipore, Schwalbach, Germany) on a semidry blotter (BioRad Laboratories, Munich, Germany). After blocking the membrane with the blocking reagent (Applichem, Darmstadt, Germany), immunoreactivity was detected with primary affinity-purified rabbit polyclonal anti-harmonin H3 (50) or mouse monoclonal anti-FLAG (Sigma-Aldrich, Hannover, Germany) and appropriate secondary antibodies (IRDye 680 or 800, Rockland) (Biotrend Chemikalien, Köln, Germany), employing the Odyssey infra red imaging system (LI-COR Biosciences, Bad Homburg, Germany). As a molecular marker, a pre-stained ladder (Sigma-Aldrich) was used, ranging from 11 to 170 kDa.

SUPPLEMENTARY MATERIAL

Supplementary Material is available at *HMG* online.

ACKNOWLEDGEMENT

We thank the Mainz University Eye Clinic, Thomas Riepert and Bianca Navarro for providing human tissue samples.

Conflict of Interest statement. None declared.

FUNDING

The work was supported by the German Research Foundation (HA 1374/7-1 to T.H. and GRK 1044 to U.W.) and the FAUN-Stiftung, Nürnberg (to U.W.).

REFERENCES

1. Elden, L.M. and Postic, W.P. (2002) Screening and prevention of hearing loss in children. *Curr. Opin. Pediatr.*, **14**, 723–730.
2. Smith, R.J.H., Bale, J.F. and White, K.R. (2005) Sensorineural hearing loss in children. *Lancet*, **365**, 879–890.
3. Morton, C.C. and Nance, W.E. (2006) Newborn hearing screening—a silent revolution. *N. Engl. J. Med.*, **354**, 2151–2164.
4. Toriello, R.J., Reardon, W. and Gorlin, R.J. (2004) *Hereditary Hearing Loss and Its Syndromes*, Oxford University Press, Oxford, UK.
5. Hone, S.W. and Smith, R.J. (2003) Genetic screening for hearing loss. *Clin. Otolaryngol.*, **28**, 285–290.
6. Kremer, H., van Wijk, E., Märker, T., Wolfrum, U. and Roepman, R. (2006) Usher syndrome: molecular links of pathogenesis, proteins and pathways. *Hum. Mol. Genet.*, **15**, R262–R270.
7. Reiners, J., Nagel-Wolfrum, K., Jürgens, K., Märker, T. and Wolfrum, U. (2006) Molecular basis of human Usher syndrome: deciphering the meshes of the Usher protein network provides insights into the pathomechanisms of the Usher disease. *Exp. Eye Res.*, **83**, 97–119.
8. Williams, D.S. (2008) Usher syndrome: animal models, retinal function of Usher proteins, and prospects for gene therapy. *Vis. Res.*, **48**, 433–441.
9. Weil, D., Küssel, P., Blanchard, S., Lévy, G., Levi-Acobas, F., Drira, M., Ayadi, H. and Petit, C. (1997) The autosomal recessive isolated deafness, DFNB2, and the Usher 1B syndrome are allelic defects of the myosin-VIIA gene. *Nat. Genet.*, **16**, 191–193.
10. Ahmed, Z.M., Smith, T.N., Riazuddin, S., Makishima, T., Ghosh, M., Bokhari, S., Menon, P.S., Deshmukh, D., Griffith, A.J., Riazuddin, S. *et al.* (2002) Nonsyndromic recessive deafness DFNB18 and Usher syndrome type IC are allelic mutations of USHIC. *Hum. Genet.*, **110**, 527–531.
11. Bork, J.M., Peters, L.M., Riazuddin, S., Bernstein, S.L., Ahmed, Z.M., Ness, S.L., Polomeno, R., Ramesh, A., Schloss, M., Srisailpathy, C.R. *et al.* (2001) Usher syndrome 1D and nonsyndromic autosomal recessive deafness DFNB12 are caused by allelic mutations of the novel cadherin-like gene CDH23. *Am. J. Hum. Genet.*, **68**, 26–37.
12. Mburu, P., Mustapha, M., Varela, A., Weil, D., El-Amraoui, A., Holme, R.H., Rump, A., Hardisty, R.E., Blanchard, S., Coimbra, R.S. *et al.* (2003) Defects in whirlin, a PDZ domain molecule involved in stereocilia elongation, cause deafness in the whirler mouse and families with DFNB31. *Nat. Genet.*, **34**, 421–428.
13. De Kok, Y.J.M., Vosenaar, E.R., Cremers, C.W., Dahl, N., Laporte, J., Hu, L.J., Lacombe, D., Fischel-Ghodsian, N., Friedman, R.A., Parnes, L.S. *et al.* (1996) Identification of a hot spot for microdeletions in patients with X-linked deafness type 3 (DFN3) 900 kb proximal to the DFN3 gene POU3F4. *Hum. Mol. Genet.*, **5**, 1229–1235.
14. Wirth, J., Nothwang, H.G., van der Maarel, S., Menzel, C., Borck, G., Lopez-Pajares, I., Brøndum-Nielsen, K., Tommerup, N., Bugge, M., Ropers, H.H. *et al.* (1999) Systematic characterization of disease associated balanced chromosome rearrangements by FISH: cytogenetically and genetically anchored YACs identify microdeletions and candidate regions for mental retardation genes. *J. Med. Genet.*, **36**, 271–278.
15. Bugge, M., Bruun-Petersen, G., Brøndum-Nielsen, K., Friedrich, U., Hansen, J., Jensen, G., Jensen, P.K., Kristoffersson, U., Lundsteen, C., Niebuhr, E. *et al.* (2000) Disease associated balanced chromosome rearrangements: a resource for large scale genotype–phenotype delineation in man. *J. Med. Genet.*, **37**, 858–865.
16. Williamson, R.E., Darrow, K.N., Michaud, S., Jacobs, J.S., Jones, M.C., Eberl, D.F., Maas, R.L., Liberman, M.C. and Morton, C.C. (2007) Methylthioadenosine phosphorylase (MTAP) in hearing: gene disruption by chromosomal rearrangement in a hearing impaired individual and model organism analysis. *Am. J. Med. Genet.*, **143A**, 1630–1639.
17. Hook, E.B. (1983) Chromosome abnormalities and spontaneous fetal death following amniocentesis: further data and association with maternal age. *Am. J. Hum. Genet.*, **35**, 110–116.
18. Warburton, D. (1991) *De novo* balanced chromosome rearrangements and extra marker chromosomes identified at prenatal diagnosis: clinical significance and distribution of breakpoints. *Am. J. Hum. Genet.*, **49**, 995–1101.
19. Khan, S.Y., Ahmed, Z.M., Shabbir, M.I., Kitajiri, S., Kalsoom, S., Tasneem, S., Shayiq, S., Ramesh, A., Srisailpathy, S., Khan, S.N. *et al.* (2007) Mutations of the RDX gene cause nonsyndromic hearing loss at the DFNB24 locus. *Hum. Mutat.*, **28**, 417–423.
20. Verhoeven, K., van Laer, L., Kirschhofer, K., Legan, P.K., Hughes, D.C., Schatteman, I., Verstreken, M., van Hauwe, P., Couke, P., Chen, A. *et al.* (1998) Mutations in the human alpha-tectorin gene cause autosomal dominant non-syndromic hearing impairment. *Nat. Genet.*, **19**, 60–62.
21. Mustapha, M., Weil, D., Chardenoux, S., Elias, S., El-Zir, E., Beckmann, J.S., Loiselet, J. and Petit, C. (1999) An alpha-tectorin gene defect causes a newly identified autosomal recessive form of sensorineural pre-lingual non-syndromic deafness, DFNB21. *Hum. Mol. Genet.*, **8**, 409–412.
22. Reiners, J., van Wijk, E., Märker, T., Zimmermann, U., Jürgens, K., te Brinke, H., Overlack, N., Roepman, R., Knipper, M., Kremer, H. *et al.* (2005) Scaffold protein harmonin (USH1C) provides molecular links between Usher syndrome type 1 and type 2. *Hum. Mol. Genet.*, **14**, 3933–3943.
23. Reiners, J., Märker, T., Jürgens, K., Reidel, B. and Wolfrum, U. (2005) Photoreceptor expression of the Usher syndrome type 1 protein protocadherin 15 (USH1F) and its interaction with the scaffold protein harmonin (USH1C). *Mol. Vis.*, **11**, 347–355.
24. Van Wijk, E., van der Zwaag, B., Peters, T., Zimmermann, U., te Brinke, H., Kersten, F.F., Märker, T., Aller, E., Hoefsloot, L.H., Cremers, C.W.

et al. (2006) The DFNB31 gene product whirlin connects to the Usher protein network in the cochlea and retina by direct association with USH2A and VLGR1. *Hum. Mol. Genet.*, **15**, 751–765.
25. Maerker, T., van Wijk, E., Overlack, N., Kersten, F.F., McGee, J., Goldmann, T., Sehn, E., Roepman, R., Walsh, E.J., Kremer, H. *et al.* (2008) A novel Usher protein network at the periciliary reloading point between molecular transport machineries in vertebrate photoreceptor cells. *Hum. Mol. Genet.*, **17**, 71–86.
26. Kleinjan, D.K. and van Heyningen, V. (2005) Long-range control of gene expression: emerging mechanisms and disruption in disease. *Am. J. Hum. Genet.*, **76**, 8–32.
27. Belloni, E., Muenke, M., Roessler, E., Traverso, G., Siegel-Bartelt, J., Frumkin, A., Mitchell, H.F., Donis-Keller, H., Helms, C., Hing, A.V. *et al.* (1996) Identification of Sonic hedgehog as a candidate gene responsible for holoprosencephaly. *Nat. Genet.*, **14**, 353–356.
28. Lettice, L.A., Heaney, S.J., Purdie, L.A., Li, L., de Beer, P., Oostra, B.A., Goode, D., Elgar, G., Hill, R.E. and de Graaff, E. (2003) A long-range Shh enhancer regulates expression in the developing limb and fin and is associated with preaxial polydactyly. *Hum. Mol. Genet.*, **12**, 1725–1735.
29. Pfeifer, D., Kist, R., Dewar, K., Devon, K., Lander, E.S., Birren, B., Korniszewski, L., Back, E. and Scherer, G. (1999) Campomelic dysplasia translocation breakpoints are scattered over 1 Mb to SOX9: evidence for an extended control region. *Am. J. Hum. Genet.*, **65**, 111–124.
30. Velagaleti, G.V.N., Bien-Willner, G.A., Northup, J.K., Lockhart, L.H., Hawkins, J.C., Jalal, S.M., Withers, M., Lupski, J.R. and Stankiewicz, P. (2005) Position effects due to chromosome breakpoints that map ~900 kb upstream and 1.3 Mb downstream of SOX9 in two patients with campomelic dysplasia. *Am. J. Hum. Genet.*, **76**, 652–662.
31. Jakobsen, L.P., Ullmann, R., Christensen, S.B., Jensen, K.E., Molsted, K., Henriksen, K.F., Hansen, C., Knudsen, M.A., Larsen, L.A., Tommerup, N. *et al.* (2007) Pierre Robin sequence may be caused by dysregulation of SOX9 and KCNJ2. *J. Med. Genet.*, **44**, 381–386.
32. Nikiforova, M.N., Stringer, J.R., Blough, R., Medvedovic, M., Fagin, J.A. and Nikiforov, Y.E. (2000) Proximity of chromosomal loci that participate in radiation-induced rearrangements in human cells. *Science*, **290**, 138–141.
33. Roix, J.J., McQueen, P.G., Munson, P.J., Parada, L.A. and Misteli, T. (2003) Spatial proximity of translocation-prone gene loci in human lymphomas. *Nat. Genet.*, **34**, 287–291.
34. Lanctôt, C., Cheutin, T., Cremer, M., Cavalli, G. and Cremer, T. (2007) Dynamic genome architecture in the nuclear space: regulation of gene expression in three dimensions. *Nat. Rev. Genet.*, **8**, 104–115.
35. Spilianakis, C.G., Lalioti, M.D., Town, T., Lee, G.R. and Flavell, R.A. (2005) Interchromosomal associations between alternatively expressed loci. *Nature*, **435**, 637–645.
36. Martinez-Castro, P., Ramos, M.C., Rey, J.A., Benitez, J. and Sanches Cascos, A. (1984) Homozygosity for a Robertsonian translocation (13q14q) in three offspring of heterozygous parents. *Cytogenet. Cell Genet.*, **38**, 310–312.
37. Eklund, A., Simola, K.O.J. and Ryynänen, M. (1988) Translocation t(13;14) in nine generations with a case of translocation homozygosity. *Clin. Genet.*, **33**, 83–86.
38. Rockman-Greenberg, C., Ray, M., Evans, J.A., Canning, N. and Hamerton, J.L. (1982) Homozygous Robertsonian translocation in a fetus with 44 chromosomes. *Hum. Genet.*, **61**, 181–184.
39. Dallapiccola, B., Ferranti, G., Altissimi, D., Colloridi, F. and Paesano, R. (1989) First-trimester prenatal diagnosis of homozygous (14;21) translocation in a fetus with 44 chromosomes. *Prenat. Diagn.*, **9**, 555–558.
40. Leschot, N.J., Velden, J., Marinkovic-Ilsen, A., Darling, S.M. and Nijenhuis, L.E. (1986) Homozygosity for a Y/22 chromosome translocation: t(Y;22)(q12;p12/13). *Clin. Genet.*, **29**, 251–257.
41. Wilmot, P.L., Shapiro, L.R. and Casamassima, A.C. (1990) Disomic balanced reciprocal translocation. *Clin. Genet.*, **28**, 126–127.
42. Martinet, D., Vial, Y., Thonney, F., Beckman, J.S., Meagher-Villemure, K. and Unger, S. (2006) Fetus with two identical reciprocal translocations: description of a rare complication of consanguinity. *Am. J. Med. Genet.*, **140A**, 769–774.
43. Zaki, M., Shehab, M., El-Aleem, A.A., Abdel-Salam, G., Koeller, H.B., Ilkin, Y., Ross, M.E., Dobyns, W.B. and Gleeson, J.G. (2007) Identification of a novel recessive RELN mutation using a homozygous balanced reciprocal translocation. *Am. J. Med. Genet.*, **143A**, 939–944.
44. D'Andrea, A.D. and Grompe, M. (2003) The Fanconi anaemia/BRCA pathway. *Nat. Rev. Cancer*, **3**, 23–34.
45. Oti, M. and Brunner, H.G. (2007) The modular nature of genetic disease. *Clin. Genet.*, **71**, 1–11.
46. Boëda, B., El-Amraoui, A., Bahloul, A., Goodyear, R., Daviet, L., Blanchard, S., Perfettini, I., Fath, K.R., Shorte, S., Reiners, J. *et al.* (2002) Myosin VIIa, harmonin and cadherin 23, three Usher I gene products that cooperate to shape the sensory hair cell bundle. *EMBO J.*, **21**, 6689–6699.
47. Ahmed, Z.M., Riazuddin, S., Riazuddin, S. and Wilcox, E.R. (2003) The molecular genetics of Usher syndrome. *Clin. Genet.*, **63**, 431–444.
48. Adato, A., Michel, V., Kikkawa, Y., Reiners, J., Alagramam, K.N., Weil, D., Yonekawa, H., Wolfrum, U., El-Amraoui, A. and Petit, C. (2005) Interactions in the network of Usher syndrome type 1 proteins. *Hum. Mol. Genet.*, **14**, 347–356.
49. Yue, Y., Grossmann, B., Holder, S.E. and Haaf, T. (2005) *De novo* t(7;10)(q33;q23) translocation and closely juxtaposed microdeletion in a patient with macrocephaly and developmental delay. *Hum. Genet.*, **117**, 1–6.
50. Reiners, J., Reidel, B., El-Amraoui, A., Boëda, B., Huber, I., Petit, C. and Wolfrum, U. (2003) Differential distribution of harmonin isoforms and their possible role in Usher-1 protein complexes in mammalian photoreceptor cells. *Invest. Ophthalmol. Vis. Sci.*, **44**, 5006–5515.